ANALYTICAL BIOCHEMISTRY 231, 210–217 (1995)

# Kinetics of Protein–Protein Interactions at the Surface of an Optical Biosensor

Paul R. Edwards,*[,1] Andrew Gill,† Denise V. Pollard-Knight,*[,2] Mike Hoare,† Philip E. Buckle,* Peter A. Lowe,* and Robin J. Leatherbarrow‡[,3]

*Fisons Applied Sensor Technology, East Bridge House, Saxon Way, Bar Hill, Cambridge, CB3 8SL, United Kingdom; †Department of Chemical and Biochemical Engineering, The Advanced Centre for Biochemical Engineering, University College London, Torrington Place, London, WC1E 7JE, United Kingdom; and ‡Department of Chemistry, Biological Chemistry, Imperial College of Science, Technology, and Medicine, South Kensington, London, SW7 2AY, United Kingdom

Received February 13, 1995

**Methods based on the use of optical biosensors have recently become available to provide a convenient means of determining the rate and equilibrium constants for bimolecular interactions between immobilized ligands and soluble ligate molecules. However, the association data that these methods provide are not always accurately described by the expected pseudo-first-order reaction mechanism, particularly when the ligand is immobilized on a dextran matrix. We show that a better description of the association data, especially at higher ligate concentrations, is achieved with a double exponential function, indicating that at least two rate-limiting processes are involved. Various models are considered in order to explain these observations: the presence of two (or more) distinct populations of immobilized ligand; a change, possibly conformational, in the immobilized ligand before or after ligate binding; or the hindrance of ligate binding to immobilized ligand. We suggest that steric hindrance caused by ligate binding to the dextran-coated sensor surface seems the most likely explanation for the observed biphasic association kinetics and that the faster initial phase should be used in order to determine association constants that can be compared to those in solution.** 

Bimolecular interaction analysis using optical biosensor technology has been commercially available since 1990 (1) and the number of publications in this field has rapidly increased (2–4). The biosensor monitors interactions between pairs of molecules, where one partner is immobilized on the surface of the sensor and the other is in solution. The advantages that these methods have over more conventional techniques include high sensitivity, real-time monitoring, and no requirement for the use of labeled material. If such measurements are to provide kinetic and equilibrium constants that can be related to interactions in solution, it is important to establish the kinetic behavior for such systems and where possible relate this to the case in solution. This is particularly important, as it has already been reported that kinetic data from optical biosensors can show deviations from that expected for interactions in free solution, with the association time course often containing more than one exponential phase (5–7).

For our investigations we used a commercially available optical biosensor based on a resonant mirror mounted in a stirred cuvette (8–10). The system was used to follow the interactions of two different model antigen–monoclonal antibody systems. These are representative of interactions that can be measured using the biosensor technique, and observations regarding binding kinetics are applicable to other like systems.

The interactions between ligand and ligate involve the equilibrium represented in Eq. [1].

$$G + L \overset{K_D}{\rightleftharpoons} GL, \qquad [GL] = \frac{[G][L]}{K_D} \qquad [1]$$

In this scheme, G represents the ligand, L the ligate, GL the associated complex, and $K_D$ the dissociation equilibrium constant. For the purposes of this paper, we shall refer to the surface-immobilized species as the ligand and the species in bulk solution as the ligate.

[1,3] To whom correspondence may be addressed.

[2] Present address: Scientific Generics Ltd., Unit D, King's Court, Kirkwood Road, Cambridge, CB4 2PF, UK.



0003-2697/95 $12.00

Under normal experimental conditions the association is expected to be pseudo-first-order, as ligate is present in excess and so effectively remains at constant concentration during the reaction. Although expected to apply generally to nonallosteric bimolecular interactions with homogeneous binding partners, several workers have observed that this simple reaction scheme is not always the case. Non-first-order kinetics have been found for ligate binding to an absorbed ligand on a planar surface by surface plasmon resonance (11) or upon ligate binding to a membrane-coated planar surface by fluorescence photobleaching (12) and to a covalently bound ligand on a dextran surface (5–7). Data for these interactions are often found to be better described by equations in which there are two time-dependent functions.

In this paper we investigate the kinetics of ligand–ligate interactions in order to model the association parameters and explain these observations. The following model associating antigen–antibody systems were used: (a) human serum albumin (HSA)[4] anti-HSA and (b) tumor necrosis factor (TNF)/anti-TNF. Antibody/antigen interactions have frequently been studied using biosensors, and so it is appropriate to use such systems as models for kinetic analysis.

## MATERIALS AND METHODS

### *Materials*

All chemicals used were of analytical reagent grade. Phosphate-buffered saline (PBS) tablets, 1,3,4,6-tetrachloro-3$\alpha$,6$\alpha$-di-phenylglycouril, and bovine serum albumin (BSA) were obtained from Sigma Chemical Co. (Poole, UK). Surfact-Amps 20 and bis(sulfosuccinimidyl)suberate (BS) were obtained from Pierce & Warriner (Chester, UK). HSA and anti-HSA were from Biogenesis Ltd. (Bournemouth, UK). TNF and anti-TNF monoclonal antibody were a gift from Cambridge Antibody Technology, Melbourn Science Park (Melbourn, UK). An amine coupling kit (containing 1-ethyl-3-(3-dimethylaminopropyl)carbodiimide (EDC), *N*-hydroxysuccinimide (NHS), and 1 M ethanolamine, pH 8.5), IAsys carboxymethyl dextran (CMD), and aminosilane cuvettes were from Fisons Applied Sensor Technology, Bar Hill (Cambridge, UK). [$^{125}$I]Sodium iodide with a specific activity of 100 mCi ml$^{-1}$ was obtained from ICN Biomedicals Inc. (Thame, UK). PBS/T buffer was prepared by the addition of 0.05% (v/v) Surfact Amps 20 to PBS buffer, pH 7.4.

[4] Abbreviations used: HSA, human serum albumin; TNF, tumor necrosis factor; BS, bis(sulfosuccinimidyl)suberate; EDC, 1-ethyl-3-(3-dimethylaminopropyl)carbdiimide; NHS, *N*-hydroxysuccinimide; CMD, carboxymethyl dextran; PBS, phosphate-buffered saline; BSA, bovine serum albumin.

### *Operation of the Optical Biosensor System*

Association measurements were made using the IAsys instrument (Fisons Applied Sensor Technology), following the procedures recommended by the manufacturer. The instrument detects changes in refractive index and/or thickness occurring within a few hundred nanometers from the sensor surface. The sensor relies upon a biomolecule being attached to the sensor surface. Ligand immobilization can be followed in "real-time" with the instrument producing a plot of response, measured in arc seconds, against time. Binding of ligate to the immobilized ligand also produces an instrument response which is again measured in arc seconds. This was performed using ligands coupled to CMD or aminosilane cuvettes, in a total volume of 200 $\mu$l. The stirred cuvette system used in this instrument ensures that mass-transport effects during binding are minimized.

### *Ligand Immobilization to the CMD Matrix*

Coupling of ligand to the CMD matrix was performed essentially as described by Davies *et al.* (10). Carboxyl groups on the dextran were activated by an EDC/NHS solution for 8 min. Following activation, the EDC/NHS mixture was replaced with PBS/T for 5 min to establish a preimmobilization baseline response on the biosensor. Immobilization was then initiated by the addition of ligand to the cuvette. The contact time for the immobilization of anti-TNF and anti-HSA was 10 min. For the HSA:anti-HSA stoichiometry investigation the contact times were varied in order to achieve a range of immobilization signals. The ligand solutions were replaced, after the set contact time, by an ethanolamine wash for 2 min to quench residual NHS esters. The cuvette was finally washed with PBS/T to establish a postimmobilization response level. The difference in the pre- and postimmobilization responses is used to calculate the amount of ligand immobilized using the relationship that 1 ng protein mm$^{-2}$ gives a response of 163 arc s on the IAsys instrument (10).

### *Ligand Immobilization to Aminosilane Surfaces*

To determine the effect of the CMD matrix upon the kinetics of ligate binding, ligand was also immobilized directly to a sensor surface lacking the CMD matrix. This direct immobilization was performed as follows. After initial preequilibration of an aminosilane cuvette with 10 mM phosphate buffer, pH 7.0, the homobifunctional crosslinker BS (1 mM) was added for 10 min. Following reequilibration with phosphate buffer, anti-HSA was immobilized at 250 $\mu$g/ml in 10 mM phosphate buffer, pH 7.0, for 10 min. Remaining activated sites were then blocked with BSA (5 mg/ml) for 10 min after which the BSA solution was replaced with phosphate buffer.

*Monitoring the Binding of Ligate to Immobilized Ligand*

Anti-TNF (10 μg/ml) or anti-HSA (10 μg/ml) was dissolved in 10 mM acetate, pH 5.0. TNF and HSA were dissolved in PBS/T. Before recording an interaction profile, the ligand-coupled cuvette was washed with the relevant regeneration buffer (i.e., 10 or 25 mM HCl for 2 min), then reequilibrated in 180 μl PBS/T. To this PBS/T, 20 μl of the appropriate ligate solution was added. For TNF binding, seven different TNF concentrations up to 200 nM were used with a contact time of 10 min. To determine the stoichiometry of HSA binding to immobilized anti-HSA, HSA (3.3 μM) was allowed to interact with the immobilized anti-HSA for 15 min. This concentration was shown to saturate the sites on the immobilized ligand. Ligate was then fully removed with a 2-min 10 mM HCl wash followed by a 5-min PBS/T reequilibration before the next binding cycle.

*Direct Measurement of Bound Ligate Using Radiolabeled HSA*

To determine that the response obtained from the instrument is directly related to the amount of ligate bound, radiolabeled HSA (3.3 μM) was allowed to bind for contact times of up to 30 min while the binding response from the sensor was recorded. HSA was labeled using 1,3,4,6-tetrachloro-3α,6α-di-phenylglycouril and $Na^{125}I$ (13) to a specific activity of 500 kBq $mg^{-1}$. The bound $^{125}I$ HSA was removed from the immobilized anti-HSA by a 2-min wash with 10 mM HCl. The amount of bound $^{125}I$ HSA was then determined by sampling a 100-μl aliquot of the acid regeneration solution and measuring the radioactivity present (Pharmacia 1282 CompuGamma). The acid wash was found to remove all the bound $^{125}I$ HSA from the CMD surfaces (data not shown).

*Kinetic Analysis of Interaction Profiles*

Data were analyzed by nonlinear regression (14–16) using the FASTfit software package supplied with the IAsys instrument. The equations to which the data were fitted are described under Theoretical Background.

## THEORETICAL BACKGROUND

For a simple bimolecular interaction of ligate with ligand, binding is described by Eq. [1] provided that there is a single binding site on the ligate. If the ligate is in excess, the amount of complex formation at time $t$, $[GL]_t$, is given by Eq. [2].

$$[GL]_t = [GL]_\infty[1 - \exp(-k_{on}t)] \quad [2]$$

In this equation, $[GL]_\infty$ is the concentration of complex at infinite time, and the pseudo-first-order rate constant for the process is $k_{on}$. For the biosensor, the change in instrument response, $R$, (measured in arc seconds) is proportional to the amount of bound ligate, giving Eq. [3].

$$R_t = (R_\infty - R_0)[1 - \exp(-k_{on}t)] + R_0 \quad [3]$$

$R_t$ is the response at time $t$, $R_0$ is the initial response, and $R_\infty$ is the maximal response.

From Eq. [3], the instrument response should increase in a single exponential manner. However, experimentally derived association data are not always well described by such a simple relationship, and data obtained from an optical biosensor frequently have at least two distinguishable phases (5–7). This biphasic association involves two distinct rate processes and can be described by Eq. [4].

$$R_t = A[1 - \exp(-k_{on(1)}t)] + B[1 - \exp(-k_{on(2)}t)] + R_0 \quad [4]$$

Here the response, $R_t$, varies with two apparent association rate constants ($k_{on(1)}$ and $k_{on(2)}$); the magnitudes of the two phases are $A$ and $B$, respectively, such that $R_\infty = R_0 + A + B$. Mechanisms that can give rise to multiphasic association data are considered in the Discussion.

The value of $k_{on}$ varies with ligate concentration as described by Eq. [5].

$$k_{on} = k_{diss} + k_{ass}[L] \quad [5]$$

A plot of $k_{on}$ against [L] allows the association constant, $k_{ass}$, to be determined from the slope and the dissociation constant, $k_{diss}$, from the intercept. However, the value of $k_{diss}$ so obtained is often close to zero and inaccurately defined. Hence, $k_{diss}$ is usually best measured directly by removing all the free ligate and allowing the GL complex to dissociate. Dissociation is observed as an exponential decay of the complex with time as described in Eq. [6].

$$[GL]_t = [GL]_0\exp(-k_{diss}t) \quad [6]$$

In this equation, the amount of complex at time $t$, $[GL]_t$, is dependent upon the initial complex concentration, $[GL]_0$, and the dissociation rate constant, $k_{diss}$. Determination of both $k_{ass}$ and $k_{diss}$ allows the calculation of the dissociation equilibrium constant, $K_D$, as shown in Eq. [7].

$$K_D = \frac{k_{diss}}{k_{ass}} \quad [7]$$

## RESULTS

### *Kinetic Analysis for the Interaction of TNF with Anti-TNF*

Experimental data obtained from the interaction between TNF and anti-TNF (immobilized on a CMD cuvette) were fitted using equations having one and two exponential terms (Eqs. [3] and [4]). In general, at all but very low concentrations of TNF, the data are poorly fitted by equations that have a single exponential term. Figure 1a shows the association recorded at 12 nM together with the best-fit single exponential curve, which is found to fit the observed response well. Figures 1b and 1c show the association at 200 nM, with best-fit single exponential (1b) and double exponential (1c) curves. At this higher concentration the single exponential fit to the data is poor, and the double exponential equation gives a much better description of the data. In each case an error plot, derived from the arithmetic difference between the fitted curve and the data, is shown.

Association constants, $k_{ass}$, were found from plots of $k_{on}$ (the apparent on-rate, produced from individual curve fits), against the relevant ligate concentration using Eq. [5]. Figure 2 shows the concentration dependence of the two apparent on-rate constants for the TNF/anti-TNF interaction.

### *Binding of $^{125}I$ HSA to Immobilized Anti-HSA*

The amount of ligand bound to the sensor surface was measured directly using $^{125}I$ HSA binding to immobilized anti-HSA and compared with the instrument response during this experiment. These studies show that the response during association phase is directly proportional to the amount of ligate bound. As shown in Fig. 3 for binding to derivatized CMD-coated surfaces, there is a linear relationship between instrument response and the amount of radioactive material bound. This relationship is maintained over the whole of the time course, even though the binding curve is biphasic. The slope of the cpm versus response curve corresponds to 206 arc s $ng^{-1}$ $mm^{-2}$, which is approximately the same as previous estimates of 163 arc s $ng^{-1}$ $mm^{-2}$ for the IAsys instrument (10).

### *Comparison of HSA Binding to Anti-HSA Immobilized on CMD and Aminosilane Cuvettes*

Figure 4 shows the binding of HSA to anti-HSA immobilized (a) to aminosilane cuvettes and (b and c) to CMD cuvettes, under otherwise identical conditions. The binding to CMD cuvettes produces a much larger change in response, but is characteristically biphasic, as the data are fitted poorly by equations with only one exponential term (b), but well by equations with two exponential terms (c) (see Discussion). For the aminosi-

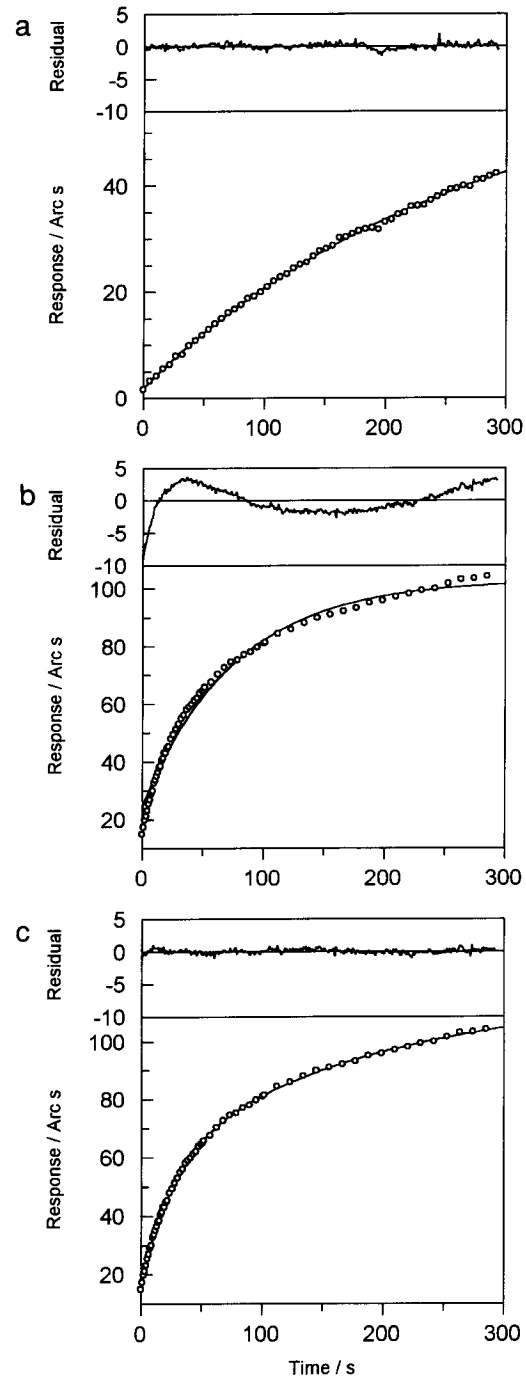


**FIG. 1.** Binding of TNF to anti-TNF immobilized to a CMD cuvette. (a) 12 nM TNF, single exponential fit. (b) 200 nM TNF, single exponential fit. (c) 200 nM TNF, double exponential fit. In each case the experimental data are the open circles, and the best-fit curves are shown as solid lines. Over the main graphs is plotted in each case the residual error, calculated as the experimental data minus the calculated. For clarity, due to the very large number of data points that are generated by the biosensor, the main graphs show only part of the complete data set. For (a), every 10th data point is shown; for (b), all points before 20 s, every 2nd data point between 20 and 50 s, every 5th point between 50 and 100 s, and every 10th above 100 s are shown.

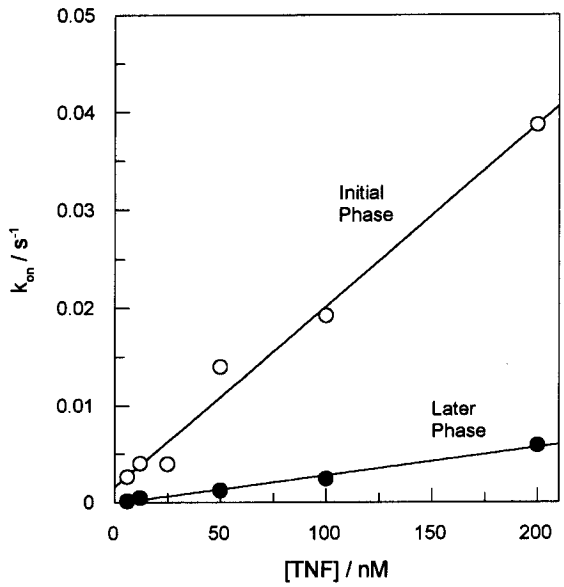


**FIG. 2.** Concentration dependence of the two $k_{on}$ values derived from double exponential curve fitting of TNF binding to anti-TNF immobilized on a CMD cuvette. (○) $k_{on(1)}$ (initial phase), (●) $k_{on(2)}$ (later phase).

lane system, virtually all of the ligand sites are occupied seconds after the addition of ligate, and the data are fitted well assuming a single binding phase. The rate constants found from these experiments are as follows (standard errors from the data fitting are given in parentheses): (a) 0.033 $s^{-1}$ (0.0006); (b) 0.091 $s^{-1}$ (0.002) and 0.0064 $s^{-1}$ (0.00008).

### *Stoichiometry of HSA Binding to Immobilized Anti-HSA*

The effect of surface ligand concentration on the measured binding stoichiometry of HSA to anti-HSA immobilized on a CMD cuvette is shown in Fig. 5. The stoichiometry is calculated as the ratio of immobilized response to binding response on a molar basis, as in Eq. [8].

$$\text{Stoichiometry} = \frac{\left(\dfrac{\text{Binding Response for HSA}}{67{,}000}\right)}{\left(\dfrac{\text{Immobilization Response for Anti-HSA}}{150{,}000}\right)} \quad [8]$$

It is found that as the concentration of immobilized ligand is lowered, the apparent stoichiometry of bound ligate increases. Extrapolation to infinite dilution gives a maximum stoichiometry of approximately 2.0 molecules of HSA per molecule of anti-HSA, which is the value expected for binding in solution.

## DISCUSSION

In the case of the TNF/anti-TNF interaction, at low ligate concentrations (12 nM), the association of ligate to CMD-immobilized ligand is fitted by a single exponential equation (Fig. 1a; Eq. [3]). However, at moderate to high ligate concentrations the data are not fitted adequately by this equation (Fig. 1b), but are well described by assuming a second association constant (Fig. 1c; Eq. [4]). So far, we have found similar effects for all other systems that we have studied when binding to ligands immobilized on CMD surfaces (for example, the same effect can be seen in the comparison of Fig. 4b with 4c). This effect seems to be intrinsic to the surface interaction and not a characteristic of the particular instrument used for these measurements, as we and others have observed the same effect using the BIAcore sensor manufactured by Pharmacia (5–7 and unpublished data).

To fit the observed data at higher ligate concentrations it is necessary to have at least two different rate processes that contribute to the association kinetics. Several models can be devised that give rise to the type

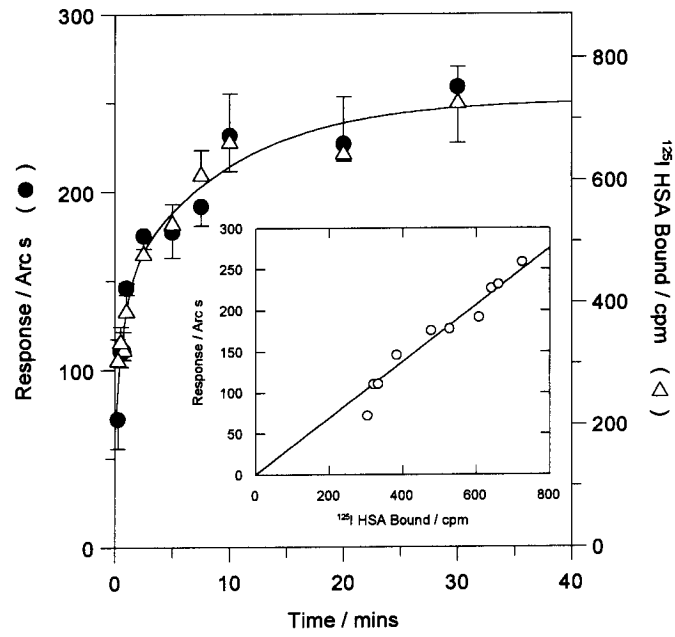


**FIG. 3.** Effect of incubation time upon the instrument response (solid circles) and amount of bound $^{125}$I HSA measured by cpm (open triangles) when binding to anti-HSA immobilized on CMD. All data points are means of triplicate values, and error bars represent the standard error of the mean (SE). The solid line shows the best fit to the data using a double exponential fit. (Inset) Relationship between cpm and instrument response. The best line through the data using linear regression is shown.

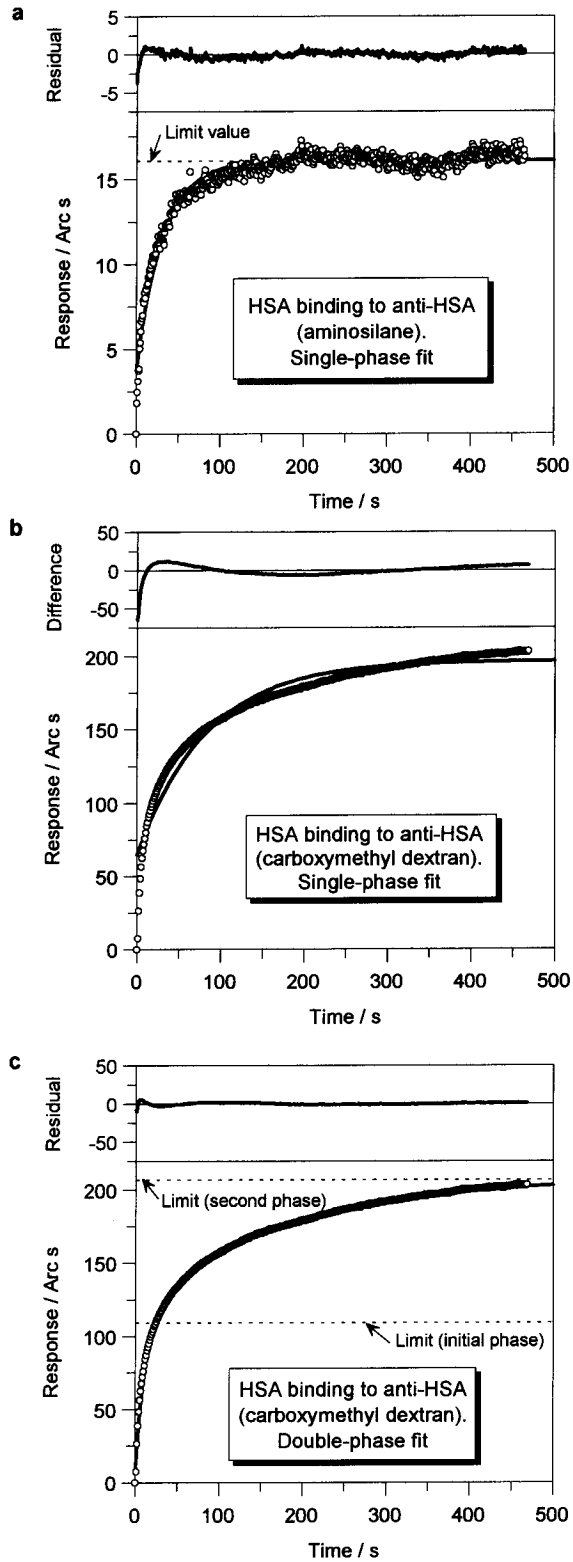


**FIG. 4.** Binding of HSA (3.7 $\mu$M) to (a) anti-HSA immobilized to an aminosilane cuvette and (b) and (c) anti-HSA immobilized to a CMD cuvette. In each case the experimental data are shown as circles, and a best-fit curve is drawn through the data points. In cases (a) and (b), this is a single exponential fit; in (c), a double exponential fit was used. In each case, over the main graphs is plotted the residual error, calculated as the experimental data minus the calculated value. The graphs (a) and (c) also show the limiting values of the different exponential phases. In (a), this is $R_\infty$ from Eq. [3], and in (c) the two limiting values are $R_0$ + A and $R_\infty$ from Eq. [4].

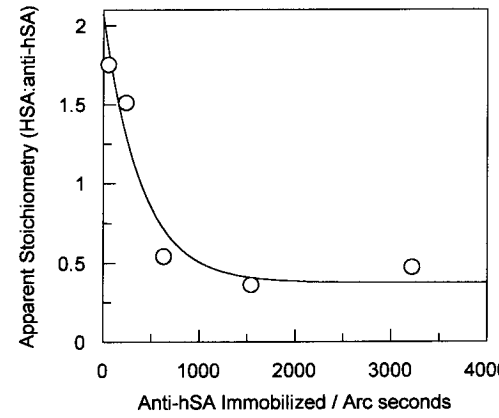


**FIG. 5.** Dependence of the binding stoichiometry between HSA and anti-HSA upon the amount of anti-HSA immobilized to the CMD cuvette.

of kinetics described by Eq. [4], and three of these are considered below.

*Possible Association-Phase Models*

*The presence of more than one type of binding site.* Several workers have considered this possibility (6, 12, 17, 18). The presence of heterogeneous binding sites could occur if the chemical immobilization process resulted in ligand with different affinities. For example, if two different binding sites were present, then two distinct binding phases would be observed (Eq. [9]).

$$G + L \underset{k_{-1}}{\overset{k_1[L]}{\rightleftharpoons}} GL \qquad G' + L \underset{k_{-1'}}{\overset{k_{1'}[L]}{\rightleftharpoons}} G'L \qquad [9]$$

The two classes of ligand are denoted G and G′. The rate of ligate binding would therefore be described by Eq. [4], with the two different association constants being $k$ and $k'$. The magnitude of the different phases would depend upon the relative proportion of the various classes of binding sites present. At low ligate concentrations, provided that the affinities of the sites were substantially different, only the high-affinity site would be occupied and so a single exponential curve could fit the experimental results. However, at high ligate concentrations all sites would be occupied, producing biphasic kinetics. It is possible to extend these considerations to the case of $n$ classes of binding sites, which would give $n$ discernible association phases.

However, in practice it would be difficult to distinguish more than two exponential phases, and none of the data examined here justify fitting to equations that have more than two exponential phases.

*The binding involves more than a single step.* Biphasic association kinetics are found in solution where there is a time-dependent step that occurs before or after the initial encounter, e.g., a conformational change (19, 20). In terms of the present system, it is conceivable that the instrument response could reflect an event after initial binding, for example, a conformational change of the ligand, the ligate, or the surface as shown in Eq. [10].

$$G + L \underset{k_{-1}}{\overset{k_1[L]}{\rightleftharpoons}} GL \underset{k_{-2}}{\overset{k_2}{\rightleftharpoons}} (GL)' \qquad [10]$$

Alternatively, the ligand and/or the surface matrix might need to undergo a slow conformational change prior to binding, possibly in order to expose hidden binding sites, as described by Eq. [11].

$$G \underset{k_{-1}}{\overset{k_1}{\rightleftharpoons}} G' + L \underset{k_{-2}}{\overset{k_2[L]}{\rightleftharpoons}} (GL)' \qquad [11]$$

Mechanisms 10 and 11 can be distinguished by the concentration dependence of the second association phase (19). For Eq. [10], the second apparent rate constant increases with increasing [L]; for Eq. [11], it decreases. Clearly the data in Fig. 2, although possibly compatible with Eq. [10], are not consistent with the scheme described by Eq. [11].

The process in Eq. [10] would involve the second rate constant reflecting events after binding rather than being due to slow binding of later ligate. It is therefore possible to test this by direct measurement of the amount of ligate bound during the association period. To be consistent with such a kinetic scheme, the ligate bound should correspond only with the faster phase. However, direct measurement of ligate binding shows that binding as well as instrument response is intrinsically biphasic (Fig. 3), which rules out this model.

*Steric hindrance of the dextran-immobilized ligand.* In the case of HSA binding to immobilized anti-HSA, the biphasic association is associated with binding to the derivatized CMD-coated surface. It is therefore possible that some property of this matrix causes the observed kinetic behavior. This is supported by the data in Fig. 4, which show that under similar conditions binding to dextran-coated surfaces generates biphasic curves, whereas binding to ligand immobilized via an aminosilane linker to the surface gives data that have only a single exponential phase. The two rate constants that can be extracted from the CMD data show that

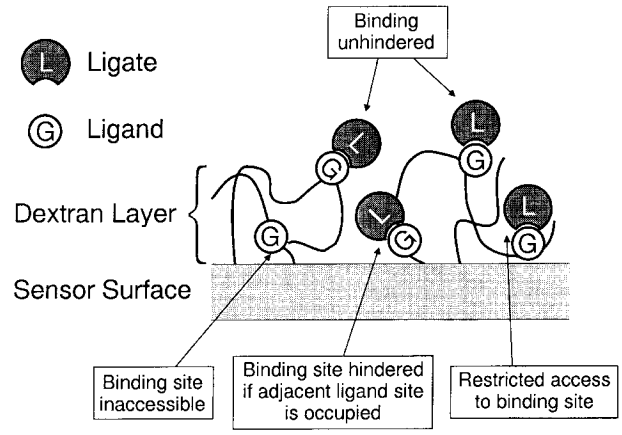


**FIG. 6.** Schematic diagram showing some of the processes that may contribute to the observed kinetic behavior when ligate binds to ligand immobilized on CMD cuvettes. Binding may be unhindered by the dextran; alternatively, the binding site may be inaccessible or present restricted access. In addition, the binding of ligate at one site may occlude binding at other sites.

the faster of the two phases is comparable to the single phase that is found when the ligand is attached to the surface more directly, using a simple aminosilane linker. It should also be noted, however, that the change in response for the former system is much larger and thus far easier to measure accurately (8,21). The surface layer of the sensor as routinely used is a carboxymethyl dextran matrix having a thickness of between 200 and 500 nm, with one carboxyl group per two glucose residues (10). Both of the currently available commercial optical biosensor instruments (the IAsys used in this study and the BIAcore manufactured by Pharmacia) use a similar surface coating. This may be expected to give a more constrained environment for ligate binding than the equivalent found in free solution. Steric hindrance can be directly demonstrated by measuring the stoichiometry of binding at different ligand concentrations (Fig. 5). The stoichiometry only approaches the expected value at very low ligand concentrations. The binding of a macromolecular ligate to ligand within the crowded matrix can be expected to restrict accessibility further, and as a consequence, binding at one ligand site could sterically hinder binding at an adjacent site. This would pose a particular problem, as complete saturation of all available sites would then need local rearrangements of ligand/ligate pairs, i.e., dissociation followed by rebinding, before all could be occupied. Interestingly, we find that the slower binding phase often has a rate constant similar to the dissociation rate constant, which could support such a view.

Hence, there are various processes that could contribute to the observed kinetics, and these are depicted in schematic form in Fig. 6. Binding to readily accessi-

ble sites will occur at a rate comparable to the situation when ligand is attached directly to the sensor surface (Fig. 4). This accounts for the fast phase of the binding profiles and should be directly comparable to the situation in free solution. We suggest that the slower binding phase could have various contributing factors and arises from restricted accessibility due to location of the immobilized ligand within the matrix and/or steric constraints imposed by binding of adjacent macromolecular ligate molecules. The equation containing two exponential terms (Eq. [4]), although empirical, describes the experimental data far better than an equation that has a single exponential term. The first rate constant in Eq. [4], $k_{ass(1)}$, represents simple association, and the variation with ligate concentration can be modeled by Eq. [5] to allow $k_{on}$ and $k_{off}$ to be determined. The second rate constant is more complex and contains no readily interpretable kinetic information. However, when analyzing association profiles obtained from an optical biosensor it is clearly important, at most concentrations, to fit the data using equations containing both one and two exponential terms. Error plots, such as shown in Fig. 1, can be useful in determining whether the equation having two exponential terms gives a better fit. Where this is the case, it is the faster rate constant that most closely mirrors binding events in solution.

## ACKNOWLEDGMENT

The authors thank Dr. Hennie Hoogenboom (Cambridge Antibody Technology, Melbourn Science Park, Melbourn, UK) for the kind donation of TNF and the anti-TNF monoclonal antibody.

## REFERENCES

1. Fägerstam, L. G., Frostell, Å., Karlsson, R., Kullman, M., Larsson, A., Malmqvist, M., and Butt, H. (1990) *J. Mol. Recognit.* **3,** 208–214.
2. Dubs, M-C., Altschuh, D., and van Regenmortel, M. H. V. (1991) *Immunol. Lett.* **31,** 59–64.
3. Felder, S., Zhou, M., Hu, P., Urena, J., Ulrich, M., Chaudhuri, M., White, M., Showlson, S. E., and Schlessinger, J. (1993) *Mol. Cell. Biol.* **13,** 1449–1455.
4. Masson, L., Mazza, A., and Brousseau, R. (1994) *Anal. Biochem.* **218,** 405–412.
5. O'Shannessy, D. J., Brigham-Burke, M., Soneson, K. K., Hensley, P., and Brooks, I. (1993) *Anal. Biochem.* **212,** 457–468.
6. Zeder-lutz, G., Altschuh, D., Geysen, H. M., Trifilieff, E., Sommermeyer, G., and van Regenmortel, M. H. V. (1993) *Mol. Immunol.* **30,** 145–155.
7. Corr, M., Slanetz, A. E., Boyd, L. F., Jelonek, M. T., Khilko, S., Al-Ramadi, B. K., Kim, Y. S., Maher, S. E., Bothwell, A. L. M., and Marguiles, D. H. (1994) *Science* **265,** 946–949.
8. Buckle, P. E., Davies, R. J., Kinning, T., Yeung, D., Edwards, P. R., Pollard-Knight, D., and Lowe, C. R. (1993) *Biosens. Bioelectron.* **8,** 355–363.
9. Cush, R., Cronin, J. M., Stewart, W. J., Maule, C. H., Molloy, J., and Goddard, N. J. (1993) *Biosens. Bioelectron.* **8,** 347–353.
10. Davies, R. J., Edwards, P. R., Watts, H. J., Lowe, C. R., Buckle, P. E., Yeung, D., Kinning, T. M., and Pollard-Knight, D. V. (1994) *in* Techniques in Protein Chemistry V, pp. 285–292, Academic Press, San Diego.
11. DeBono, R. F., Krull, U. J., and Rounaghi, G. (1992) ACS Symposium Series 511 (Mathewson, P. R., and Finley, J. W., Eds.), Chap. 11, American Chemical Society, Washington, DC.
12. Pearce, K. H., Hiskey, R. G., and Thompson, N. L. (1992) *Biochemistry* **31,** 5983–5995.
13. Fracker, R. J., and Speck, J. C. (1978) *Biophys. Res. Commun.* **80,** 849–857.
14. Motulsky, H. J., and Ransnas, L. A. (1987) *FASEB J.* **1,** 365–374.
15. Leatherbarrow, R. J. (1990) *Trends Biol. Sci.* **15,** 455–458.
16. Johnson, M. L. (1992) *Anal. Biochem.* **206,** 215–225.
17. Mach, H., Volken, D. B., Burke, C. J., Middaugh, C. R., Linhardt, R. J., Fromm, J. R., and Loganathan, D. (1993) *Biochemistry* **32,** 5480–5489.
18. Bondeson, K., Frostell-Karlsson, Å., Fägerstam, L., and Magnusson, G. (1993) *Anal. Biochem.* **214,** 245–251.
19. Fersht, A. (1985) Enzyme Structure and Mechanism, Freeman, New York.
20. Kelley, R. F., and O'Connell, M. P. (1993) *Biochemistry* **10,** 6828–6835.
21. Löfås, S., and Johnsson, B. (1990) *J. Chem. Soc. Chem. Commun.* 1526–1528.